

## Microcontact Printing of Dendrimers, Proteins, and Nanoparticles by Porous Stamps

Huaping Xu,<sup>†‡</sup> Xing Yi Ling,<sup>†</sup> Joost van Bennekom,<sup>‡</sup> Xuexin Duan,<sup>†</sup>  
Manon J. W. Ludden,<sup>†</sup> David N. Reinhoudt,<sup>†</sup> Matthias Wessling,<sup>‡</sup>  
Rob G. H. Lammertink,<sup>\*‡</sup> and Jurriaan Huskens<sup>\*†</sup>

*Molecular Nanofabrication Group, MESA+ Institute for Nanotechnology, University of Twente, P.O. Box 217, 7500AE Enschede, The Netherlands, and Membrane Technology Group, MESA+ Institute for Nanotechnology, University of Twente, P.O. Box 217, 7500AE Enschede, The Netherlands*

Received September 25, 2008; E-mail: j.huskens@utwente.nl; r.g.h.lammertink@tnw.utwente.nl

**Abstract:** Porous stamps fabricated by one-step phase separation micromolding were used for microcontact printing of polar inks, in particular aqueous solutions of dendrimers, proteins, and nanoparticles. Permanent hydrophilicity was achieved without any additional treatment by tailored choice of the polymer components. Pores with several hundred nanometers to micrometers were obtained during the phase separation process. These pores can act as ink reservoirs. The porous stamps were thoroughly characterized by SEM, NMR, and contact angle measurement. The versatility of the porous stamps was shown in three printing schemes. First, positive microcontact printing was achieved by printing a polar thioether-modified dendrimer as the ink, followed by backfilling and wet etching. Second, the porous stamps were used for multiple printing of fluorescent proteins without reinking. Third, nanoparticles of about 60 nm in diameter, which cannot be directly transferred by oxidized PDMS stamps, were successfully printed onto substrates by using these porous stamps.

### Introduction

Among all of the soft lithographic patterning techniques, microcontact printing ( $\mu$ CP) which employs a micropatterned stamp to print molecules as an ink to a surface, has proven to be a most versatile surface modification method in materials as well as in life science applications. For  $\mu$ CP, poly(dimethylsiloxane) (PDMS) elastomer has been widely used as a stamp material to generate motifs and structures ranging from about 100 nm to micrometers, owing to its advantages like conformal contact with solid substrates, optical transparency, and chemical inertness.<sup>1</sup>

In the past few years, a lot of work has been done to improve the low mechanical stability of PDMS and to solve the ink diffusion problem. This includes the fabrication of hard-PDMS<sup>2</sup> and composite stamps,<sup>3,4</sup> the development of chemically patterned flat stamps to avoid stamp collapse,<sup>5–7</sup> and the use of

high-molecular-weight inks or catalytic  $\mu$ CP to overcome ink diffusion.<sup>8–10</sup> Besides the mechanical properties, the wetting behavior of the PDMS surface is also an important issue in printing a variety of functional materials. The low-surface-energy PDMS has been used advantageously in the microcontact printing of nonpolar inks such as alkanethiols and silanes onto metal and oxides surfaces, respectively. However, surface modification is required to print polar inks such as biomolecules to facilitate cell growth, to improve biocompatibility for bioanalytical detections, etc., since the nontreated PDMS surface is hydrophobic, which is unsuited for the adsorption of such ink molecules onto the stamp surface.<sup>1</sup> The simplest approach to prepare a hydrophilic PDMS stamp for  $\mu$ CP is probably to oxidize its surface by oxygen plasma treatment, but stamps hydrophilized this way do not remain hydrophilic for a long time. Mobile, low-molecular-weight silicone residues migrate from the bulk to the air–stamp interface, which leads to the recovery of the hydrophobic character of the PDMS surface in a few hours after plasma treatment, unless the stamps are carefully stored under water.<sup>11–13</sup> In order to gain permanent hydrophilicity, a range of methods have been developed, e.g.,

- (7) van Poll, M. L.; Zhou, F.; Ramstedt, M.; Hu, L.; Huck, W. T. S. *Angew. Chem., Int. Ed.* **2007**, *46*, 1–5.
- (8) Liebau, M.; Huskens, J.; Reinhoudt, D. N. *Adv. Funct. Mater.* **2001**, *11*, 147–150.
- (9) Li, X. M.; Péter, M.; Huskens, J.; Reinhoudt, D. N. *Nano Lett.* **2003**, *3*, 1449–1453.
- (10) Perl, A.; Péter, M.; Ravoo, B. J.; Reinhoudt, D. N.; Huskens, J. *Langmuir* **2006**, *22*, 7568.
- (11) Ferguson, G. S.; Chaudhury, M. K.; Biebuyck, H. A.; Whitesides, G. M. *Macromolecules* **1993**, *26*, 5870–5875.
- (12) Fritz, J. L.; Owen, M. J. *J. Adhesion* **1995**, *54*, 33–45.

<sup>†</sup> Molecular Nanofabrication Group.

<sup>‡</sup> Membrane Technology Group.

- (1) (a) Xia, Y.; Whitesides, G. M. *Angew. Chem., Int. Ed.* **1998**, *37*, 550.  
(b) Gates, B. D.; Xu, Q. B.; Stewart, M.; Ryan, D.; Willson, C. G.; Whitesides, G. M. *Chem. Rev.* **2005**, *105*, 1171. (c) Michel, B.; Bernard, A.; Bietsch, A.; Delamarche, E.; Geissler, M.; Juncker, D.; Kind, H.; Renault, J.-P.; Rothuizen, H.; Schmid, H.; Schmidt-Winkel, P.; Stutz, R.; Wolf, H. *IBM J. Res. Dev.* **2001**, *45*, 697–719.
- (2) Schmid, H.; Michel, B. *Macromolecules* **2000**, *33*, 3042.
- (3) Bietsch, A.; Michel, B. *J. Appl. Phys.* **2000**, *88*, 4310–4318.
- (4) Menard, E.; Bilhaut, L.; Zaumseil, J.; Rogers, J. A. *Langmuir* **2004**, *20*, 6871–6878.
- (5) Geissler, M.; Bernard, A.; Bietsch, A.; Schmid, H.; Michel, B.; Delamarche, E. *J. Am. Chem. Soc.* **2000**, *122*, 6303–6304.
- (6) Sharpe, R. B. A.; Burdinski, D.; Huskens, J.; Zandvliet, H. J. W.; Reinhoudt, D. N.; Poelsema, B. *J. Am. Chem. Soc.* **2005**, *127*, 10344.

oxygen plasma or UV/ozone treatment and subsequent chemical attachment of silanes or grafting hydrophilic polymers on PDMS surfaces.<sup>14–17</sup> Plasma-induced polymerization and surface-initiated atom-transfer radical polymerization have also been explored to tune the PDMS surface properties.<sup>18–20</sup> The thus-formed hydrophilic polymer layer on the stamps was sufficient to adsorb small polar inks.

Unlike the printing of small apolar ink molecules such as alkanethiols, which can be absorbed inside the stamp and then be transferred upon contact between the stamp and substrate, the printing of high-molecular-weight inks is much more difficult due to their larger size. Such inks cannot be absorbed by the stamps but merely adhere to the stamps' outer surface. Therefore, reinking is necessary after every step.<sup>1</sup> Some hydrophilic materials with a so-called "ink reservoir" function have been fabricated by different groups. Micropatterned hydrogels such as agarose and polyacrylamide were recently reported to deliver controllable quantities of chemicals onto or into a variety of supports.<sup>21–24</sup> Yet only small ionic inorganic species were taken up by the hydrogels. Whether sufficiently large entities such as proteins or nanoparticles can go inside the hydrogel stamps is yet unclear. For the direct and multiple printing of such polar inks, new stamp materials and methods need to be developed.

Recently, a new approach for microstructuring various polymer-based materials called phase separation micromolding (PS $\mu$ M) was developed.<sup>25,26</sup> PS $\mu$ M is a convenient and versatile microfabrication technique that can be used to structure a broad range of polymers, including block copolymers, and biodegradable and conductive polymers, without the need of cleanroom facilities. The method relies on the phase separation of a polymer solution while in contact with a structured mold. Phase separation on a mold mostly results in porosity in a microstructured polymer product which will endow the polymer membrane with many functionalities; for example, the pore structures can act as a scaffold for cell attachment and tissue formation.<sup>27</sup>

Here, we report on the successful  $\mu$ CP of aqueous ink solutions of dendrimers, proteins, and nanoparticles by porous

microstructured stamps fabricated by PS $\mu$ M using the pore structures as "ink reservoirs". This is the first example of using porous materials as a stamp for  $\mu$ CP. Because the ink is absorbed inside the porous structures, even multiple printings of proteins and nanoparticles become possible without the need for reinking of the stamp.

## Experimental Section

**Materials and Substrate Preparation.** Poly(etherimide) (PEI, Ultem 1000, General Electric), poly(ether sulfone) (PES, BASF Ultrason E6020P), poly(vinylpyrrolidone) (PVP, Fluka, K30 (mw = 30 000), K90 (mw = 360 000)), *N*-methylpyrrolidone (NMP, Acros), *N*-[3-(trimethoxysilyl)propyl]ethylenediamine (TPEDA, Aldrich), and 16-mercaptohexadecanoic acid (MHDA, Aldrich) were used as received. Second-generation dendritic dialkyl sulfide (G2S) was synthesized as described previously.<sup>10</sup> The functionalization of the Fc fragment of human immunoglobulin (HIgG-Fc, Sigma-Aldrich) with rhodamine was performed according to literature procedures.<sup>28,29</sup> After labeling, the protein:rhodamine ratio was approximately 1:2. Preparation of  $\beta$ -cyclodextrin (CD)-functionalized 60 nm silica nanoparticles was performed as described previously.<sup>30,31</sup> Molds with 20 and 5  $\mu$ m wide trenches used to fabricate the porous stamps were made by silicon micromachining. Gold substrates were obtained from Ssens BV (Hengelo, The Netherlands) as a layer of 20 nm gold on titanium (2 nm) on silicon. Prior to use, SiO<sub>2</sub>/Si and glass slides were cleaned and activated by immersion in piranha (3:1 ratio of concd H<sub>2</sub>SO<sub>4</sub> and 33 wt% H<sub>2</sub>O<sub>2</sub>, CAUTION! Piranha solutions should be handled with great care in open containers in a fume hood. Piranha is highly corrosive, toxic, and potentially explosive) for 30 min and rinsing with substantial amounts of water.

**Porous Stamp Fabrication.** PEI/PVP and PES/PVP blends with different weight percentages were dissolved in NMP by stirring for 72 h. Unless indicated otherwise, the polymer and solvent weight percentage ratio was PEI:PVP:NMP = 18%:12%:70% and PES:PVP:NMP = 15%:10%:75% for PEI and PES, respectively. The polymer solutions were cast on the mold using a casting knife and then directly immersed in water. The casting height was typically several hundred micrometers. After phase separation and release from the mold, the resulting sheets were left in water for 2 h to ensure thorough solvent exchange. Subsequently, the polymer films were dried at room temperature. For SEM measurements, the porous films were completely dried in vacuum.

**Porosity Measurement.** The porosity of the porous stamps can be quantified according to following equation:<sup>27</sup>

$$\text{porosity (\%)} = \frac{\text{bulk volume (m}^3\text{)} - \text{skeletal volume (m}^3\text{)}}{\text{bulk volume (m}^3\text{)}} \times 100 \quad (1)$$

where

$$\text{bulk volume (m}^3\text{)} = \text{width (m)} \times \text{length (m)} \times \text{thickness (m)} \quad (2)$$

$$\text{skeletal volume (m}^3\text{)} = \text{weight (g)} / \text{density (g}\cdot\text{m}^{-3}\text{)} \quad (3)$$

The density of the polymers was determined by a pycnometer (Micromeritics Accupyc 1330), and the thickness of the porous film was measured by SEM.

- (13) Delamarche, E.; Bernard, A.; Schmid, H.; Michel, B.; Biebuyck, H. A. *Science* **1997**, *276*, 779–781.
- (14) Olander, B.; Wirsén, A.; Albertsson, A.-C. *J. Appl. Polym. Sci.* **2004**, *91*, 4098–4104.
- (15) Efimenko, K.; Wallace, W. E.; Genzer, J. J. *Colloid Interface Sci.* **2002**, *254*, 306–315.
- (16) Hu, S.; Ren, X.; Bachman, M.; Sims, C. E.; Li, G. P.; Allbritton, N. *Anal. Chem.* **2002**, *74*, 4117–4123.
- (17) Delamarche, E.; Donzel, C.; Kamounah, S. S.; Wolf, H.; Geissler, M.; Stutz, R.; Schmidt-Winkel, P.; Michel, B.; Mathieu, H. J.; Schaumburg, K. *Langmuir* **2003**, *19*, 8749–8758.
- (18) He, Q.; Liu, Z.; Xiao, P.; Liang, R.; He, N.; Lu, Z. *Langmuir* **2003**, *19*, 6982–6986.
- (19) Sadhu, V. B.; Perl, A.; Péter, M.; Rozkiewicz, D. I.; Engbers, G.; Ravoo, B. J.; Reinhoudt, D. N.; Huskens, J. *Langmuir* **2007**, *23*, 6850.
- (20) Azzaroni, O.; Moya, S. E.; Brown, A. A.; Zheng, Z.; Donath, E.; Huck, W. T. S. *Adv. Funct. Mater.* **2006**, *16*, 1037–1042.
- (21) Fialkowski, M.; Campbell, C. J.; Bensemman, I. T.; Grzybowski, B. A. *Langmuir* **2004**, *20*, 3513.
- (22) Klajn, R.; Fialkowski, M.; Bensemman, I. T.; Bitner, A.; Campbell, C. J.; Bishop, K. J. M.; Smoukov, S.; Grzybowski, B. A. *Nat. Mater.* **2004**, *3*, 729.
- (23) Mayer, M.; Yang, J.; Gitlin, I.; Gracias, D. H.; Whitesides, G. M. *Proteomics* **2004**, *4*, 2366.
- (24) Coq, N.; van Bommel, T.; Hikmet, R. A.; Stapert, H. R.; Dittmer, W. U. *Langmuir* **2007**, *23*, 5154–5160.
- (25) Vogelaar, L.; Barsema, J. N.; van Rijn, C. J. M.; Nijdam, W.; Wessling, M. *Adv. Mater.* **2003**, *15*, 1385.
- (26) Vogelaar, L.; Lammertink, R. G. H.; Barsema, J. N.; Nijdam, W.; Bolhuis-Versteeg, L. A. M.; van Rijn, C. J. M.; Wessling, M. *Small* **2005**, *1*, 645.

- (27) Papenburg, B. J.; Vogelaar, L.; Bolhuis-Versteeg, L. A. M.; Lammertink, R. G. H.; Stamatiadis, D.; Wessling, M. *Biomaterials* **2007**, *28*, 1998.
- (28) Brinkley, M. *Bioconjugate Chem.* **1992**, *3*, 2–13.
- (29) Holmes, K. L.; Lantz, L. M. *Methods in Cell Biology, Chapter 9: Protein Labeling with Fluorescent Probes*; Academic Press: New York, 2001; pp 185–204.
- (30) Mahalingam, V.; Onclin, S.; Péter, M.; Ravoo, B. J.; Huskens, J.; Reinhoudt, D. N. *Langmuir* **2004**, *20*, 11756.
- (31) Ling, X. Y.; Huskens, J.; Reinhoudt, D. N. *Langmuir* **2006**, *22*, 8777.

**$\mu$ CP of Polar Inks.** The porous stamps were stuck onto a device generating reduced pressure on the backside and then inked with a few drops of a polar ink solution (aqueous solution of dendrimers, proteins, or nanoparticles). After full wetting of the stamps, reduced pressure was applied to trap the ink inside the porous stamps. Reduced pressure was achieved by a two-headwater flow pipe and was kept for several min. Trace amounts of water should be left on the stamp surface to achieve reliable printing. After release of the pressure, the surfaces of the stamps were dried in a nitrogen stream. The substrates were then put in contact with the porous stamps by applying a pressure of around 200 g/cm<sup>2</sup>.

**Dendrimer as Ink.** For dendrimer G2S (aqueous solution, 10<sup>-5</sup> M) as ink and ODT (10<sup>-4</sup> M in ethanol) as backfilling, the duration of printing on gold substrates was 30 s and the dipping time in the ODT solution was 30 s. The patterned gold substrates were etched in a Fe(III)/thiourea etching bath (10 mM Fe(NO<sub>3</sub>)<sub>3</sub>, 15 mM thiourea, and 1.2% HCl) for 2.5 min at 45 °C and washed thoroughly by water and dried in a nitrogen stream.

**Proteins as Ink.** Prior to printing, a TPEDA layer was assembled onto the glass substrates by vapor deposition.<sup>32</sup> When printing fluorescent proteins (0.01 mM in PBS buffer, pH = 7.5) using porous stamps, the contact time was 5 min. In the control experiment, PDMS stamps were prepared from commercially available Sylgard-184 poly(dimethyl siloxane) (Dow Corning). The curing agent and the prepolymer were manually mixed in a 1:10 volume ratio and cured overnight at 60 °C. After peel-off from the master, the PDMS stamps were oxidized by exposure of the surface to a Telpa 300E microwave oxygen plasma for 30 s. The newly oxidized PDMS stamps were stored under water.

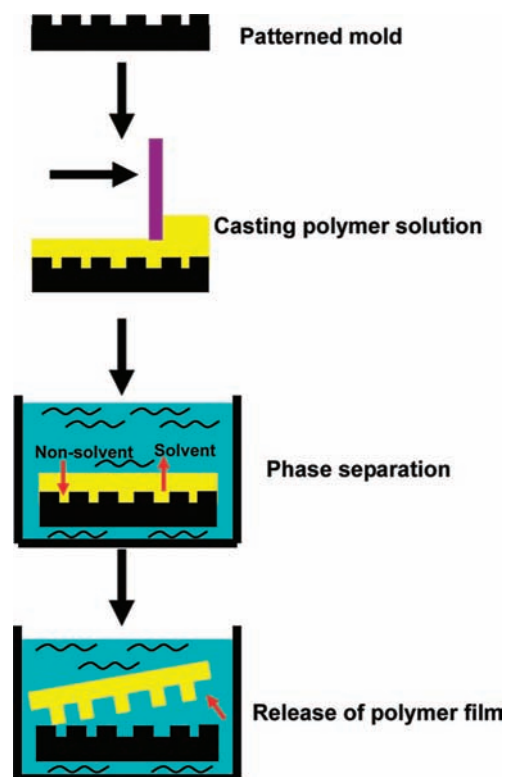
**Nanoparticles as Ink.**  $\beta$ -Cyclodextrin (CD)-functionalized silica nanoparticles (1.25% w/w) were dispersed in aqueous carbonate buffer (pH = 9.2). Prior to printing, TPEDA was assembled onto the freshly oxidized silica substrates by vapor deposition. An MHDA monolayer was assembled onto gold substrates by immersion in 1 mM MHDA in ethanol solution for 8 h. The printing time was 5 min.

**Analysis.** For the SEM measurements of the porous stamps, 5 nm of Au was coated to facilitate the SEM observation. All SEM images were taken with a HR-LEO 1550 FEG SEM or JSM 5600 LV. Contact angles were measured on a Krüss G10 contact angle setup equipped with a CCD camera. Advancing and receding contact angles were determined automatically during growth and reduction of a clean water droplet by the droplet shape analysis routine. AFM analyses were carried out with a NanoScope III (Veeco/Digital Instruments, Santa Barbara, CA) multimode atomic force microscope equipped with a J-scanner, in contact mode by using Si<sub>3</sub>N<sub>4</sub> cantilevers (Nanoprobes, Veeco/Digital Instruments) with a nominal spring constant of about 0.32 N m<sup>-1</sup>. Fluorescence microscopy was performed using an Olympus inverted research microscope IX71 equipped with a mercury burner U-RFL-T as light source and a digital camera Olympus DP70 (12.5 million-pixel cooled digital color camera) for image acquisition. Red emission light was filtered using a U-MWG Olympus filter cube. <sup>1</sup>H NMR spectra were recorded on a Varian AC300 spectrometers, and the solvent used was CDCl<sub>3</sub>.

## Results and Discussion

**Porous Stamp Fabrication and Characterization.** PS $\mu$ M is a convenient microfabrication technique to structure polymers, especially for high  $T_g$  polymers which are difficult to shape by mechanical processing. We used the PS $\mu$ M process for the fabrication of porous structured films. Scheme 1 depicts the PS $\mu$ M process. The process starts with a polymer blend of poly(ethersulfone) (PES) and poly(vinylpyrrolidone) (PVP) or of poly(etherimide) (PEI) and PVP, which is first dissolved in *N*-methylpyrrolidone (NMP). The addition of the water-soluble

**Scheme 1.** A Schematic Representation of the Phase Separation Micromolding Process

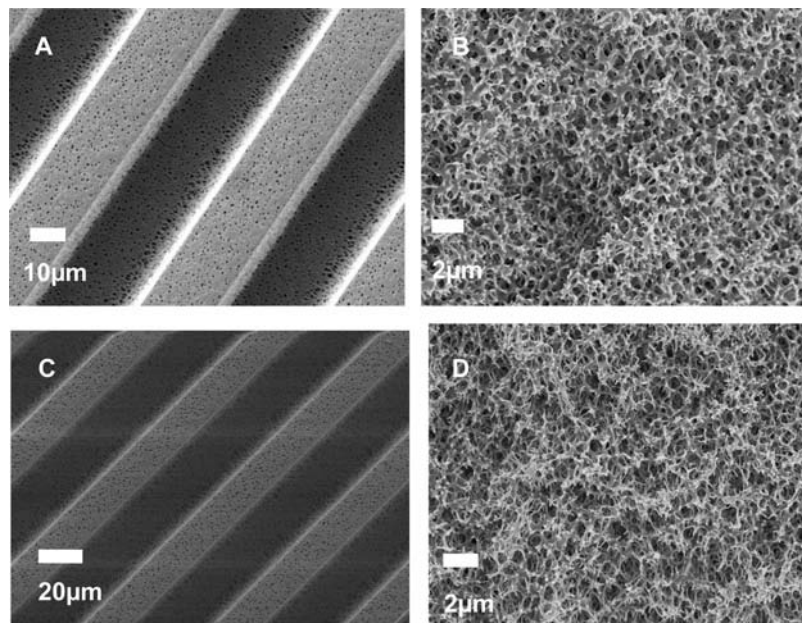


polymer PVP not only endows the stamp with hydrophilicity but also helps to yield a more uniform, interconnected pore network throughout the microstructure.<sup>26</sup> A thin film of the concentrated polymer solution was then applied on a mold by casting. Subsequently, the polymer solution was solidified by immersion in the nonsolvent water. During the solidification, the polymer assimilated the profile of the mold. After a few minutes immersion in the nonsolvent, the microstructured porous polymer film was spontaneously released from the mold.

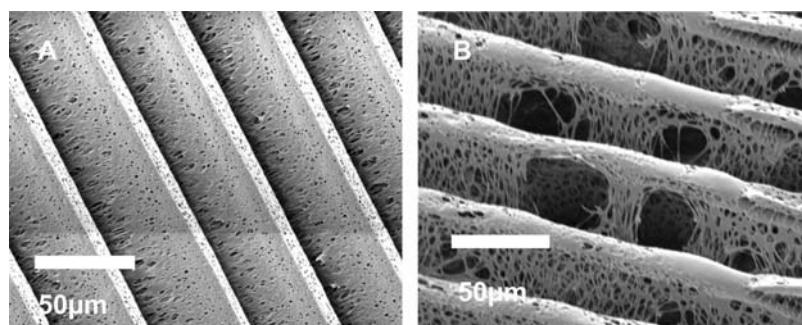
Scanning electron microscopy (SEM) was used to characterize the surface and inner morphology of the porous stamps. Figure 1 shows the SEM images of the porous microstructure of PEI/PVP and PES/PVP films. Judging from the images, only limited shrinkage happened during the solidification of the PEI/PVP polymer blend. The width of the protrusion of the porous stamps is around 19.6  $\mu$ m, compared with the 20  $\mu$ m wide trenches of the mold, and the shrinkage is only approximately 2%. However, for the PES/PVP porous stamps, around 20% of shrinkage occurred after phase separation. Since the shrinkage was uniform and predictable,<sup>26</sup> the deformation of the structure can be taken into account by the mold design so that the resulting polymer replica has the desired shape. The diameter of the pores (Figure 1B,D) is around several hundred nanometers. Only very few reach 1–2  $\mu$ m. As seen from the cross-section images, the pore structures are interconnected, which is crucial for ink entrapment and transfer during the microcontact printing process. The porosities of PEI/PVP and PES/PVP stamps were measured to be 79% and 56%, respectively.

A porous material can be imbibed with a wetting liquid because of capillary forces. When the contact angle of the liquid with the matrix material is below 90°, it will spontaneously penetrate into a porous material because of capillary pressure. In order to get an accurate value of the water contact angle, flat porous stamps were replicated directly from a smooth silicon

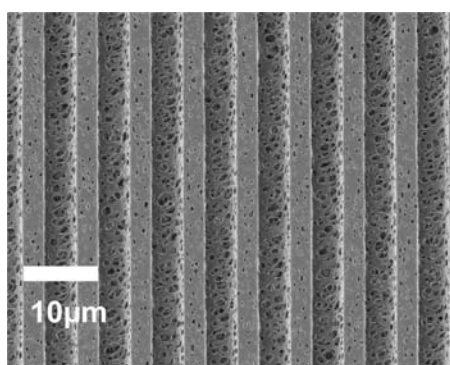
(32) Vaidya, A. A.; Norton, M. L. *Langmuir* **2004**, *20*, 11100.



**Figure 1.** Scanning electron micrographs of porous stamps replicated from a silicon mold with 20  $\mu\text{m}$  wide lines: (A, B) Surface and cross-section images of PEI/PVP (in solution PEI:PVP:NMP = 18%:12%:70% w/w); (C, D) surface and cross-section images of PES/PVP (in solution PES:PVP:NMP = 15%:10%:75% w/w).



**Figure 2.** Scanning electron micrographs of PEI/PVP porous stamps replicated from a mold with 20  $\mu\text{m}$  wide lines: A: PEI:PVP:NMP = 15%:15%:70% w/w; B PEI:PVP:NMP = 12%:8%:80% w/w.



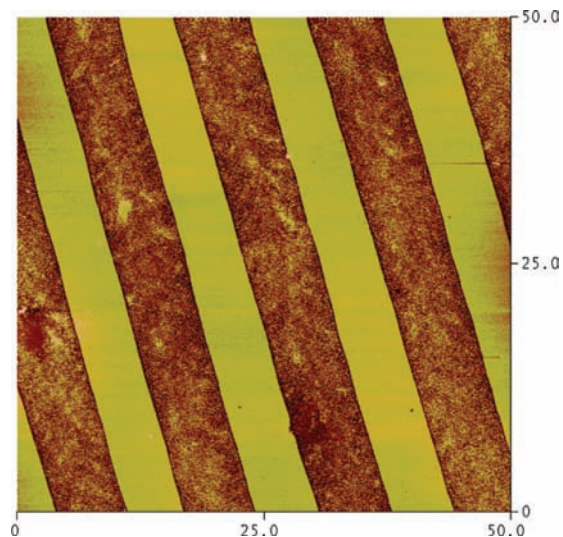
**Figure 3.** Scanning electron micrographs of PEI/PVP porous stamps, replicated from a mold with 3  $\mu\text{m}$  wide lines, PEI:PVP:NMP = 18%:12%:70% w/w.

plate without any patterns. For PEI/PVP, the flat porous stamps showed an advancing contact angle of  $53^\circ$  and a receding one of  $20^\circ$ , while for PES/PVP an advancing contact angle of  $77^\circ$  and a receding one of  $41^\circ$  were found, which means that both materials are suitable candidates for the printing of polar inks. Compared with the most commonly used oxidized PDMS stamps for polar inks, which are only temporarily hydrophilic

after the treatment of an  $\text{O}_2$  plasma, the hydrophilicity of the porous stamps is permanent, thus making it a promising material for the printing of polar inks.

For a better understanding of the  $\text{PS}\mu\text{M}$  process, it is important to know the composition of the polymer blends in the dry porous stamp. Before  $\text{PS}\mu\text{M}$ , the weight ratio of PEI and PVP in the polymer solution is 60%:40%. During the phase-separation process, part of the water-soluble PVP goes into the water phase, and the weight ratio of PEI and PVP in the dry porous stamps became 97.2%:2.8% (based on the integral ratio of the two polymers measured by NMR). Similarly for the PES/PVP porous stamps, the weight ratio of PES and PVP was 91.2%:8.8% after drying, compared with the 60%:40% ratio in the polymer solution. The small portion of the hydrophilic polymer PVP left in the porous stamps renders the stamps hydrophilic.

Many parameters influence the porosity and pore morphology of the polymer sheets obtained by immersion precipitation, e.g., the coagulation bath, the polymer composition in the polymer blends, and the polymer solution concentration. For fabrication of the PES/PVP porous stamps, the films do not easily detach from the mold when the coagulation bath is merely water. However, addition of NMP (30% in volume ratio) to the



**Figure 4.** AFM image of etched gold patterns produced by  $\mu$ CP (30 s) of G2S (aqueous solution, 0.01 mM) using a porous stamp with 5  $\mu$ m line features, backfilling with ODT (0.1 mM in ethanol, 30 s), and wet etching in a Fe(III)/thiourea etching bath (2.5 min at 45  $^{\circ}$ C).

coagulation bath reduces the deformation during the phase separation process. A slight change of ratio between the polymers and the solvent resulted in a huge difference in the appearance of the porous stamps. Homogeneous, interconnected porous structures were achieved when the solution

mixture was PEI:PVP:NMP = 18%:12%:70%. However, when the recipe was changed to PEI:PVP:NMP = 15%:15%:70%, strong shrinkage (around 65%) of the stamp after phase separation was observed (Figure 2A). The increase of the fraction of hydrophilic PVP may lead to more release of PVP into the water. Decrease of the polymer concentration speeds up the solvent exchange process between NMP and water, leading to defects in the stamp (macrovoids). When the polymer concentration was diluted to PEI:PVP:NMP = 12%:8%:80%, some macroscopic voids are seen (Figure 2 B), besides the substantial shrinkage of the stamp.

Besides the lithographic techniques used for fabrication of the mold, the minimum feature size of the replica also depends on the pore size of the structure. The biggest pore size of the polymer stamps is about 2  $\mu$ m. Smaller feature sizes down to a few micrometers were obtained with the PEI/PVP polymer blend (Figure 3). It is believed that the resolution of the porous stamp could reach below 1  $\mu$ m if the pore size is well controlled.

**Microcontact Printing Using Porous Stamps.** Porous stamps were tested for their potential application in  $\mu$ CP for the transfer of polar inks, especially with high molecular weights. First, the water-soluble second-generation poly(propylene imine) (PPI) dendrimer with eight short dialkyl sulfide ( $\text{CH}_3\text{SCH}_2$ ) end groups (G2S) was used as the ink for positive microcontact printing.<sup>10</sup> G2S was printed on a gold surface with porous PEI/PVP stamps to form line-patterned dendrimer SAMs. Thereafter, the sample was immersed in an octadecanethiol (ODT) solution to form an etch-protective SAM on the rest of the surface. After printing

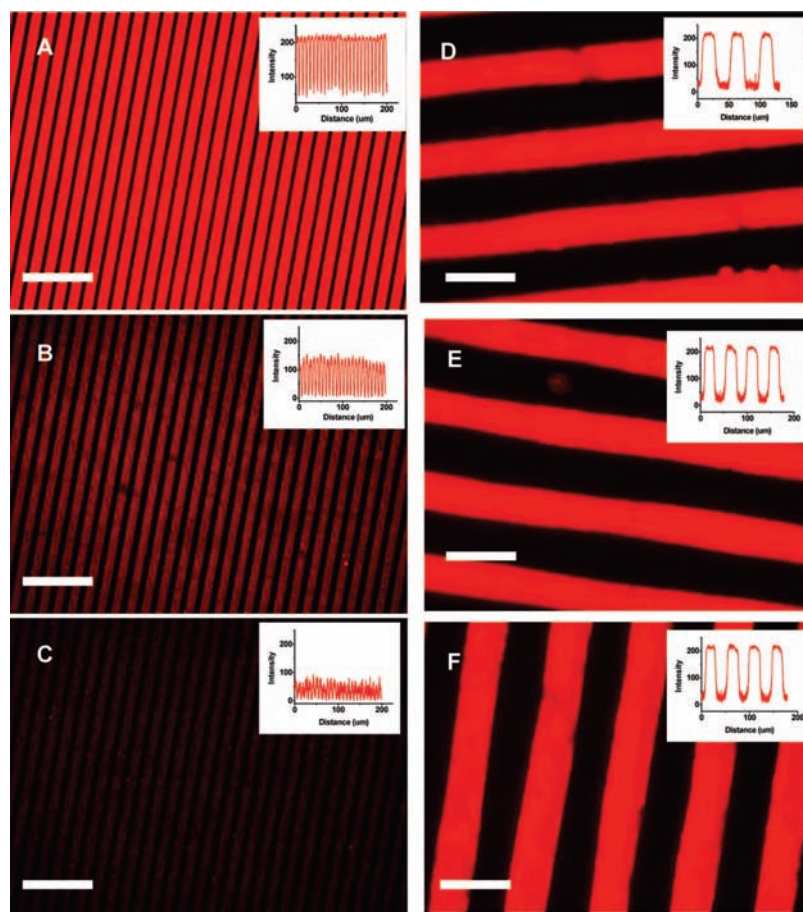


**Figure 5.** Fluorescence microscopy images (scale bars indicate 40  $\mu$ m) and intensity profiles (insets) of HlgG-Fc ( $10^{-5}$  M, PBS buffer) printed on TPEDA-functionalized glass slides in first to third prints using an oxidized PDMS stamp (A–C) and first to third prints using a porous PES/PVP stamp (D–F). Printing time was 5 min, and no reinking was used.

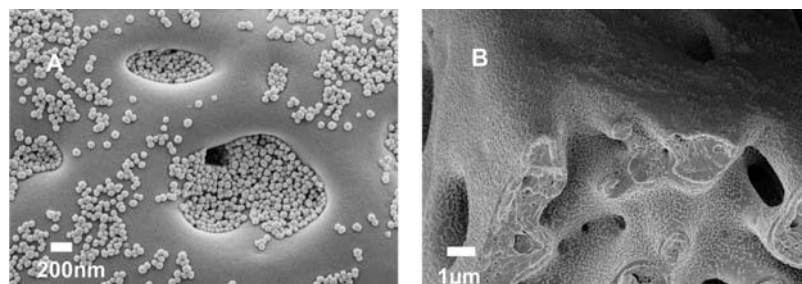


**Figure 6.** SEM surface (A) and cross-section images (B) of 60 nm  $\beta$ -cyclodextrin-functionalized SiO<sub>2</sub> nanoparticles trapped inside a porous PES/PVP stamp.

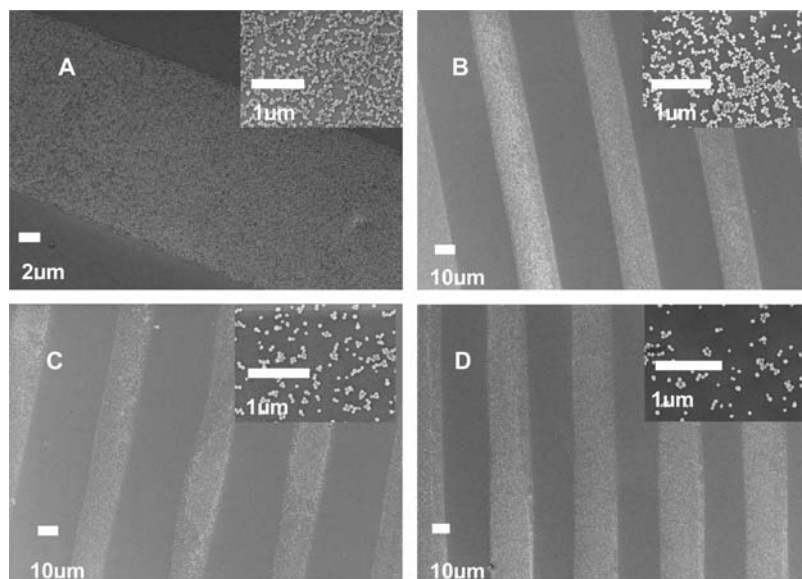


**Figure 7.** Scanning electron micrographs after  $\mu$ CP of 60 nm  $\beta$ -cyclodextrin-functionalized SiO<sub>2</sub> nanoparticles on an amino-functionalized SiO<sub>2</sub>/Si substrate using a porous PES/PVP stamp: (A–D) first to fourth printed samples using the same stamp without reinking. Insets show zoomed-in images of the contacted areas.

and backfilling, the gold substrates were etched in an acidic thiourea-based etch bath. The gold underneath the dendrimer areas was etched away to give the positive pattern of the original master. Figure 4 shows the AFM image of etched gold substrates by  $\mu$ CP of G2S by using the porous PEI/PVP stamp. The darker part is the area that was etched away by the acidic solution, while the lighter part is the area that was occupied by the backfilling molecule ODT. The line patterns of the stamps were faithfully reproduced, which indicates that the dendrimer G2S was successfully transferred to the gold substrate.

The immobilization of proteins on solid surfaces is desirable for applications such as protein arrays for biosensors, diagnostic immunoassays, and other analytical procedures.<sup>33–35</sup> For  $\mu$ CP of proteins, treated and untreated PDMS are widely used as stamp materials because of their elastomeric properties. Owing to their big size, proteins cannot be absorbed by the stamps but only adhere to the stamps' outer surface. Typically more than 90% of the proteins are transferred to the substrate during a first printing step.<sup>35</sup> Therefore reinking is necessary after every step. This prohibits easy automation for fast and large area printing.

PES/PVP porous stamps were used to investigate the possibility of multiple protein printing. PES/PVP porous stamps showed better conformal contact with the substrates than PEI/PVP porous stamps, and the former therefore commonly resulted in large-area (several cm<sup>2</sup>) printing yields. For visualization by optical fluorescence microscopy, an Fc fragment of a human immunoglobulin (HIgG-Fc) was labeled with a fluorescent marker and used as ink (0.01 mM in PBS buffer, pH = 7.5) for  $\mu$ CP. An amino-terminated SAM of *N*-[3-(trimethoxysilyl)propyl]ethylenediamine (TPEDA) was applied onto a glass slide, so that the electrostatic interaction between the proteins and the positively charged substrate provides affinity between the ink and the substrate. As a reference, experiments were also carried out with a freshly oxidized PDMS stamp. In this case, patterns can be clearly seen upon the first printing (Figure 5A). The fluorescence intensity decreased dramatically; however, upon the second printing step without reinking (Figure 5B), which means that most of the ink has been transferred to the substrate during the first printing step. Upon a third printing (Figure 5C), the fluorescence intensity decreased further and only a very faint pattern can be seen. When using a porous PES/PVP stamp, several drops of HIgG-Fc ink solution were dropped onto the stamp for imbibing. Reduced pressure was applied to the backside of the stamp, not only to trap the protein ink inside the voids of the stamp but also to prevent the microstructures (i.e., the line pattern) themselves to be filled

(33) Sauer, S.; Lange, B. M. H.; Gobom, J.; Nyarsik, L.; Seitz, H.; Lehrach, H. *Nat. Rev. Genet.* **2005**, *6*, 465–476.

(34) Bernard, A.; Renault, J. P.; Michel, B.; Bosshard, H. R.; Delamarche, E. *Adv. Mater.* **2000**, *12*, 1067–1070.

(35) Bernard, A.; Delamarche, E.; Schmid, H.; Michel, B.; Bosshard, H. R.; Biebuyck, H. *Langmuir* **1998**, *14*, 2225–2229.

by the liquid. After drying of the stamp, a glass substrate was put in contact with the stamp for 5 min under pressure. Upon a first printing step (Figure 5D), line patterns were clearly observed on the glass substrate, giving direct evidence of the transfer of HlgG-Fc from the stamp to the substrate. With the porous stamps, even multiple prints without reinking is possible, as indicated by the equal fluorescence intensity of the second and third prints (Figure 5E,F). This indicates that in the case of the porous stamps, the proteins are trapped inside the pores of the stamps and are transferred to the substrate upon contacting.

The patterning of nanoparticles is of great significance in current and future technologies such as photovoltaics, switches, LEDs, electronic data-storage systems, and sensors.<sup>36,37</sup> In all examples of employing the direct printing of nanoparticles, commonly using poly(dimethylsiloxane) (PDMS) stamps, the nanoparticle diameter is around 20 nm or below.<sup>38–41</sup> For larger size nanoparticles it is difficult to form homogeneous layers on protruding parts of the stamp. The direct printing of larger size nanoparticles is therefore still a challenge.

Negatively charged  $\beta$ -cyclodextrin (CD)-functionalized silica nanoparticles<sup>30,31</sup> with a diameter of around 60 nm were dispersed in a carbonate buffer (pH = 9.2). The nanoparticles were trapped into the pores of the porous PES/PVP stamps. As shown in Figure 6, some nanoparticles adhered to the surface of the stamp, while most of the nanoparticles were trapped inside the pores of the stamp. This proves the “ink reservoir” function of the pores for storing a nanoparticle ink solution.

The negatively charged 60 nm silica nanoparticles were printed onto amino-functionalized substrates. A TPEDA mono-

layer was applied onto freshly oxidized silicon to ensure the affinity between the negatively charged nanoparticles and the positively charged substrate. Regular  $\mu$ CP of the 60 nm nanoparticles with a freshly oxidized PDMS stamp was unsuccessful. In contrast, the successful  $\mu$ CP using the porous PES/PVP stamps is shown in Figure 7A. Clear edges can be seen between the border areas of the contacted and noncontacted areas. As indicated in the zoomed-in SEM image, the nanoparticles are not densely packed on the substrate. This is attributed to a lack of packing of the nanoparticles either on the surface or inside the porous stamps, and to the electrostatic interactions preventing the formation of ordered arrays.<sup>42</sup>

As seen in Figure 7B–D, multiple prints of nanoparticles with the same porous stamp was achieved without reinking. The layer of nanoparticles adhering to the stamp's outer surface is transferred from the stamp to the substrate during the first print. The successful second, third, and fourth prints without reinking indicate that the nanoparticles which are trapped inside the pores are transferred to the outer surface during multiple printing.

## Conclusions

Hydrophilic porous PEI/PVP and PES/PVP stamps were successfully fabricated through a convenient microfabrication technique (PS $\mu$ M). The structures of the porous stamps were influenced by variation of the polymer blends, the concentration, and the composition of the blends. By using the porous materials as stamps, high-molecular-weight polar inks (G2S, HlgG-Fc protein, and nanoparticles) were successfully transferred from the stamps to the substrates. With the pore structures functioning as ink reservoirs, multiple printing steps of HlgG-Fc and nanoparticles were achieved without reinking of the stamps. This line of research will open new avenues for the direct patterning of large and complex entities (e.g., for microarrays and biodetectors).

**Acknowledgment.** We are grateful for the financial support from the Strategic Research Orientation Nanofabrication of the MESA+ Institute for Nanotechnology, University of Twente, The Netherlands. We also thank Mark Smithers for the high-resolution SEM measurements.

JA807611N

- (36) (a) Alivisatos, A. P. *Science* **1996**, *271*, 933. (b) Fendler, J. H. *Nanoparticles and Nanostructured Films: preparation, characterization and applications*; Wiley-VCH: Weinheim, 1998. (c) Schmid, G. *Nanoparticles: From Theory to Application*; Wiley-VCH: Weinheim, Germany, 2004; p 1.
- (37) (a) Palacin, S.; Hildber, P. C.; Bourgoin, J.-P.; Miramond, C.; Fermon, C.; Whitesides, G. M. *Chem. Mater.* **1996**, *8*, 1316. (b) Larsen, N. B.; Biebuyck, H.; Delamarche, E.; Michel, B. *J. Am. Chem. Soc.* **1997**, *119*, 3017. (c) Vossmeier, T.; Delonno, E.; Heath, J. R. *Angew. Chem., Int. Ed.* **1997**, *36*, 1080. (d) Liu, X.; Fu, L.; Hong, S.; Dravid, V. P.; Mirkin, C. A. *Adv. Mater.* **2002**, *14*, 231. (e) Yin, Y.; Xia, Y. *J. Am. Chem. Soc.* **2003**, *125*, 2048. (f) Maury, P.; Escalante, M.; Reinhoudt, D. N.; Huskens, J. *Adv. Mater.* **2005**, *17*, 2718.
- (38) Li, X. M.; Paraschiv, V.; Huskens, J.; Reinhoudt, D. N. *J. Am. Chem. Soc.* **2003**, *125*, 4279.
- (39) Wu, X. C.; Bittner, A. M.; Kern, K. *Adv. Mater.* **2004**, *16*, 413.
- (40) Santhanam, V.; Andres, R. P. *Nano Lett.* **2004**, *4*, 41.
- (41) Kraus, T.; Malaquin, L.; Schmid, H.; Riess, W.; Spencer, N. D.; Wolf, H. *Nat. Nanotechnol.* **2007**, *2*, 570.

- (42) Ling, X. Y.; Malaquin, L.; Reinhoudt, D. N.; Wolf, H. *Langmuir* **2007**, *23*, 9990–9999.